One-Electron Reduction of an "Extended Viologen" *p*-Phenylene-bis-4,4′-(1-aryl-2,6-diphenylpyridinium) Dication

Alison Funston,[†] James P. Kirby,[†] John R. Miller,[†] Lubomír Pospíšil,[‡] Jan Fiedler,[‡] Magdaléna Hromadová,[‡] Miroslav Gál,[‡] Jaroslav Pecka,[§] Michal Valášek,[§] Zbigniew Zawada,[∥] Pawel Rempala,[∥] and Josef Michl*,[∥]

*Chemistry Department, Brookhaven National Laboratory, Building 555A, Upton, New York 11973,
J. Heyrovský Institute of Physical Chemistry, Academy of Sciences of the Czech Republic, Dolejškova 3,
18223 Prague, Department of Organic Chemistry, Charles University, Albertov 2030, Prague, Czech Republic,
and Department of Chemistry and Biochemistry, University of Colorado, Boulder, Colorado 80309-0215*

Received: June 29, 2005; In Final Form: September 6, 2005

One-electron reduction of the "extended viologen" dication **1** yields the red cation radical **2**, characterized by strong near-IR absorption. It has been generated and studied by pulse radiolytic, electrochemical, redox titration, UV–visible, and electron paramagnetic resonance spectroscopic methods. All results are in agreement with a fully delocalized electronic structure for **2**.

Introduction

For studies related to molecular electronics, we recently synthesized[1] potential molecular wires of five well-defined lengths. They are salts of well-defined oligomers of the *p*-phenylene-bis-4,4′-(1-aryl-2,6-diphenylpyridinium) dication **1**, with several different choices of terminal groups (Scheme 1). For obvious reasons, we refer to this unit as "extended viologen". In the oligomers, the extended viologen units are separated by aromatic rings twisted out of plane, which partially interrupt conjugation and make it likely that the transport of an electron that has been doped into the molecular wire will occur by hops from a unit to its neighbors. Charge transfer across long conjugated molecular wires is likely to occur by the hopping mechanism in any event, but our structure has been designed to force the hops to take place between structurally predefined units.[2]

The spectroscopic and electrochemical characterization of **1** doped with a single electron are a prerequisite for a meaningful study of the longer oligomers and are the subject of the present paper. We have examined several derivatives differing in the substituents located in the para positions of the terminal aryls. These rings are strongly twisted out of the pyridinium plane, and although they participate in the description of electronic excitation in **1**,[1] the nature of the terminal substituent has little effect on redox properties. Most of the reported work was performed on the bisacetamido derivatives **1a**.

Of particular interest to us is the issue of charge and spin delocalization between the two equivalent halves of the singly reduced extended viologen **2**, since it will determine the size of the units among which an electron doped into the molecular wire will hop. The existence of two symmetry-related resonance structures for **2**, in which an electron has been added to one or the other pyridinium ring of the dication (Scheme 1), suggests two possibilities. Not counting rotamers, one is a single minimum in the potential energy surface (delocalized structure,

SCHEME 1

X = NHCOCH₃   **a**
    NH₂   **b**
    N(CH₃)₂   **c**
    H   **d**
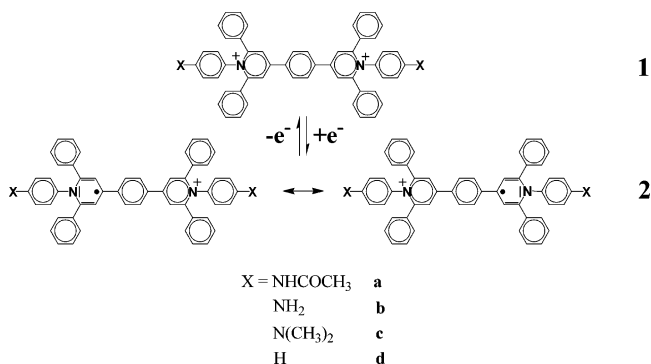
"mixed valence species"). The other possibility is two minima with localized structures, hence a rapidly interconverting pair of equivalent structures.

Polymers based on the extended viologen unit **1** have been known for some time.[3–5] It has been reported[6] that UV irradiation of these polymers and of the model monomeric compound **1d** in amide solvents such as DMF destroys their characteristic absorption peak at 342 nm and produces a red-colored species with an absorption peak near 500 nm, assigned as a product of photoreduction, presumably the radical cation **2d**. Continued irradiation causes complicated reactions and destroys the polymers.

Similar extended viologens have also been used for the preparation of soluble polyimides[7] and as agents for charge transport across vesicles.[8] The structurally closely related ordinary viologens have been studied in much more detail, and some of the interest was related to the design of molecular electronic devices.[9–11] Their redox behavior is very rich, and structural similarity to **1** suggests a similar degree of complexity in our case. A typical viologen is the dimethyl derivative, methyl viologen (paraquat). All related analogous dications undergo a facile reversible one-electron reduction[12–17] to a blue cation radical, which can be further reversibly reduced to a neutral form. Similar reversible two-step reduction was also observed for several alkyl chain separated bis-pyridinium[18] or 4,4′-bipyridinium[19–21] derivatives. Reduction is often coupled with

One-Electron Reduction of an Extended Viologen

J. Phys. Chem. A, Vol. 109, No. 48, 2005 **10863**

a strong adsorption[22−29] on both mercury and noble metals. Two-dimensional condensation and reorientation effects were found in a nonaqueous medium for viologen carrying a heptyl chain.[30] The reduced molecules readily undergo chemical reactions among themselves or serve as electron transfer mediators. The dimerization of the cation radical[13,31−34] has a rate constant[35,36] close to 10^4 M^{-1} s^{-1}. In a comproportionation[37] reaction, the dication and the neutral species produce two molecules of the radical cation. Very fast comproportionation was found to cause migration effects at low ionic strengths.[38,39] A complex set of chemical reactions was found when methyl viologen reacts with the hydrogen atom.[40]

Experimental Section

Materials. The synthesis of a series of salts of the dications **1a**, **1b**, and **1d** has been described,[1] and the preparation of **1c** is given below. The salts used in pulse radiolytic and chemical reduction experiments contained the $CB_{11}Me_{12}^-$ counterion, and those used for electrochemistry were triflates. Tetrabutyl-ammonium hexafluorophosphate (Aldrich), used as the supporting electrolyte, was recrystallized twice from ethanol and vacuum-dried. Acetonitrile (Fluka) and dimethylsufoxide (Aldrich) were dried over a freshly activated molecular sieve. In some experiments, the molecular sieve was added to all compartments of an electrochemical cell. In Prague, tetra-hydrofuran was refluxed with potassium and distilled under argon prior to use. At Brookhaven and in Boulder, THF and THF-d_8 were distilled from sodium-benzophenone under argon and acetonitrile (MeCN) was distilled and stored under argon. All subsequent manipulations of THF avoided contact with the ambient atmosphere.

Synthesis. General Procedures. Analytical samples were dried at $100−120$ °C under reduced pressure (1.4 Pa) and stored in a desiccator over P_2O_5. NMR spectra were recorded on a Varian INOVA-400 spectrometer at 25 °C in DMSO-d_6. ^1H NMR (400 MHz) spectra were referenced to TMS. ^{13}C NMR (100.58 MHz) with total decoupling of protons was referenced against the solvent (DMSO-d_6, δ 31.5 ppm; CF$_3$COOD, δ 161.35 ppm). Signal multiplicity was determined by DEPT, and the assignment of some protons was done by HSQC and HMBC experiments. For ^{19}F NMR (376.29 MHz) spectra, CF$_2$Cl$_2$ was used as an external standard. ESI-MS spectra were measured on a Bruker Esquire 3000 instrument (samples dissolved in MeCN). IR spectra were measured in KBr matrix by diffuse reflectance with a Magna 760 FTIR spectrometer (Nicolet). UV−vis spectra were measured on an Agilent 8453 spectro-photometer in acetonitrile in a 1 cm quartz cell at 20 °C. The melting points were determined with a Boëtius micromelting point apparatus and are uncorrected. Elemental analyses were performed using a Perkin-Elmer 2400 II instrument.

1,4-Bis[1-(4-*N,N*-dimethylaminophenyl)-2,6-diphenyl-pyridinium-4-yl]benzene (1c) Triflate. To the solution of *p*-phenylene-bis-4,4′-(2,6-diphenylpyrylium) triflate[5] (500 mg, 0.60 mmol) in dry dimethylformamide (12 mL) *N,N*-dimethyl-*p*-phenylenediamine (179 mg, 1.31 mmol) was added, and the mixture was stirred and heated at 60 °C. After 2 h, dry benzene (4 mL) was added and water was distilled off using a Dean−Stark trap at 120 °C. Then, the solution was stirred and heated to 120 °C for 8 h. After cooling, the solvents were evaporated (1.4 Pa, 40 °C) and the crude product was stirred with toluene (5 mL). The dark solid was filtered and washed with chloroform (3 × 10 mL) and extracted in small Soxhlet extraction apparatus with diethyl ether (50 mL). The yield of the brown product was 0.42 g (89%). ^1H NMR (DMSO-d_6): δ 2.78 (s, 12H), 6.39 (d,

4H), 7.14 (d, 4H), 7.41−7.46 (m, 20H), 8.61 (s, 4H), 8.77 (s, 4H). ^{13}C NMR: δ 110.27, 119.44, 125.59, 127.37, 128.09, 128.94, 129.63, 129.77, 133.47, 136.64, 149.86, 153.26, 157.13, 160.06. ^{19}F NMR: δ −77.29 (s). IR (KBr): ν cm^{-1} 3060 [bw, ν(CH), pyridinium and arom.], 2893 [m, ν_s(CH$_3$)], 2806 [m, ν(CH$_3$)], 1622 [s, ν(C−C), pyridinium and arom.], 1520 [s, ν(C−C), arom.], 1266 [vs, ν_{as}(SO$_3^-$)], 1156 [bs, ν(CF$_3$)], 1064 [w, ν_{as}(CNC)], 1029 [vs, ν_s(SO$_3^-$)], 835 [w, ν_s(CNC)], 821 [m, δ(CH), phenylene], 702 and 637 [m, δ(CH), Ph]. UV (λ_{max}/nm, ϵ): 326 (56000), 268 (37000). ESI-MS *m/z* (%) 388.4 (100, [M − 2A]$^{2+}$). Anal. calcd for C$_{58}$H$_{48}$F$_6$N$_4$O$_6$S$_2$ (1075.14): C, 64.79; H, 4.50; N, 5.21. Found: C, 65.11; H, 4.39; N, 5.43.

Conversion to Salt of CB$_{11}$Me$_{12}^-$. The lithium salt of dodecamethyl-carba-*closo*-dodecaborate[41] (1.5 equiv of Li$^+$CB$_{11}$-Me$_{12}^-$ per starting anion) was added to a solution of triflate in acetonitrile. This solution was stirred for 0.5 h and then an excess of water was added. The precipitate was filtered off, washed twice with water and with benzene, and then dried under reduced pressure overnight. The yield was quantitative. The resulting solid was checked by negative ESI-MS for the presence of CB$_{11}$Me$_{12}^-$ anion (*m/z* = 311.5) and absence of triflate TfO$^-$ (*m/z* = 149.0) or by ^{19}F NMR (CD$_3$CN) for the absence of fluorine signals and by ^1H NMR (CD$_3$CN) for the presence of methyl signals: 0.787 [s, 3H, CH$_3$(1)], −0.370 [s, 15H, CH$_3$(2−6)], −0.465 [s, 15H, CH$_3$(7−11)], and −0.568 [s, 3H, CH$_3$(12)].

2,4,6-Triphenylpyrylium Triflate. A suspension of tri-phenylmethanol (937 mg, 3.6 mmol) in acetic anhydride (10 mL) was stirred and maintained at 5 °C in a ice bath, while TfOH (50% in distilled water, 675 mg, 4.5 mmol) was added carefully and slowly. 1,3,5-Triphenyl-1,5-pentanedione[42,43] (1.0 g, 3.0 mmol) was then added. After the mixture was stirred for 6 h, the yellow precipitate that formed was collected by filtration, subsequently washed with acetic anhydride (2 × 20 mL), toluene (10 mL), and Et$_2$O (15 mL), and dried overnight at 120 °C under reduced pressure to afford 1.34 g (97%) of a fluorescing yellow powder; mp 256−258 °C. ^1H NMR (CF$_3$COOD): δ 7.68−7.74 (m, 6H), 7.78−7.83 (m, 3H), 8.12 (d, 2H), 8.29 (d, 4H), 8.57 (s, 2H). ^{13}C NMR (CF$_3$COOD): δ 109.72, 112.54, 113.60, 115.35, 118.17, 127.36, 127.79, 128.05, 129.70, 129.81, 132.09, 135.31, 135.49, 167.21, 171.43. IR (KBr): ν cm^{-1} 3067 [bw, ν(CH), pyrylium and arom.], 2849 (bw), 2748 (bw), 1622 [s, ν(C−C), pyrylium and arom.], 1594 [m, ν(C−C), arom.], 1499 [s, ν(C−C), arom.], 1276 (vs), 1263 [vs, ν_{as}(SO$_3^-$)], 1139 [bm, ν(CF$_3$)], 1032 [s, ν_s(SO$_3^-$)], 999 [w, ν(C−C), pyrylium], 873 [m, δ(CH), phenylene], 766 and 639 [m, δ(CH), Ph]. UV (λ_{max}/nm, ϵ): 405 (30000), 353 (31000), 277 (18000). ESI-MS *m/z* (%): 309.2 (100, [M − A]$^+$). Anal. calcd for C$_{24}$H$_{17}$F$_3$O$_4$S (458.45): C, 62.88; H, 3.74. Found: C, 63.09; H, 3.82.

1-[4-(Acetylamino)phenyl]-2,4,6-triphenylpyridinium (3) Triflate. To the solution of 2,4,6-triphenylpyrylium triflate (1 g, 2.2 mmol) in dry dimethylformamide (5 mL), *p*-amino-acetanilide (706 mg, 4.7 mmol) was added and the mixture was stirred and heated at 60 °C. After 2 h, dry benzene (2 mL) was added and water was distilled off using Dean−Stark trap at 120 °C. The solution was stirred and heated to 120 °C for the next 5 h. After the solution was cooled, the solvents were evaporated (1.4 Pa, 40 °C) and the solid was heated under reflux in toluene (20 mL) for 30 min. After the mixture was cooled, it was filtered and washed with chloroform (10 mL) and diethyl ether (100 mL) and dried at 120 °C under reduced pressure. The yield of light yellow product was 1.17 g (90%); mp 267−269 °C. ^1H NMR (DMSO-d_6): δ 1.97 (s, 3H), 7.37−7.40 (m, 15H), 7.68 (d, 2H), 8.36 (d, 2H), 8.66 (s, 2H), 10.00 (s, 1H). ^{13}C NMR: δ 117.76, 125.13, 128.12, 128.81, 129.12, 129.69, 129.90, 132.47,

133.19, 133.45, 133.49, 140.08, 155.39, 156.53, 168.78, 169.28. IR (KBr): ν cm^{-1} 3313 [bw, ν(NH)], 3061 [bw, ν(CH), pyridinium and arom.], 1692 (m, amide I), 1623 [s, ν(C−C), pyridinium and arom.], 1535 (bm, amide II), 1512 [m, ν(C−C), arom.], 1250 [bs, ν_{as} (SO$_3$$^-$)], 1167 [bm, ν(CF$_3$)], 1031 [s, ν_s(SO$_3$$^-$)], 849 [m, δ(CH), phenylene], 764 and 696 [m, δ(CH), Ph]. UV (λ_{max}/nm, ϵ): 308 (32000), 248 (23000). ESI-MS m/z (%): 441.4 (100, [M − A]$^+$). Anal. calcd for C$_{32}$H$_{25}$F$_3$N$_2$O$_4$S (590.61): C, 65.08; H, 4.27; N, 4.74. Found: C, 65.23; H, 4.19; N, 4.82.

Pulse Radiolysis. These experiments were carried out at the Brookhaven National Laboratory's Laser-Electron Accelerator Facility (LEAF). The facility[44] and methods[45] have been described. An electron pulse of <50 ps width was focused into a quartz cell with an optical path length of 5 or 20 mm containing the solution of interest. The monitoring light source was a 75 W Osram pulsed xenon arc lamp pulsed to a few hundred times its normal intensity. Wavelengths were selected using either 40 or 10 nm interference filters. Transient absorption signals were detected with either an FND-100Q silicon diode (EG&G) for λ < 1000 nm or a GAP-500L InGaAs diode (Germanium Power Devices) for λ > 1000 nm and digitized with a Tektronix TDS-680B oscilloscope. The transmission/time data were analyzed with Igor Pro software (Wavemetrics).

The total dose per pulse was determined before each series of experiments by measuring the change in absorbance of the electron in water. The dose received was calculated using ϵ (700 nm, e_{aq}^-) = 18830 M^{-1} cm^{-1} and $G(e_{aq}^-)$ = 2.97. The dose was corrected for the difference in electron density of the organic solvents used as compared to that of water. Radiolytic doses of 5−18 Gy were employed. Solutions in THF or THF-d_8 were prepared in an argon environment and sealed under argon with rubber septa or Teflon vacuum stoppers. Samples were prepared immediately prior to use. During irradiation, samples were exposed to as little UV light as possible to avoid photodecomposition, although no evidence of this occurring was found within the time frames monitored. Measurements were carried out at 22 °C.

Chemical Reduction. Sodium reductions were carried by distilling sodium metal under vacuum into the sidearm of a 2 mm cell containing **1a**. THF was stored over sodium−potassium alloy and distilled into the cell under vacuum from the alloy. The cell was sealed, and a solution of **1a** was allowed to contact the sodium mirror for 10 s at a time. A UV−vis−NIR spectrum was taken after each 10 s interval. Reductions by cobaltocene (CoCp$_2$) were performed under argon. A spectrophotometric cell was filled in a glovebox and closed with a septum. Its spectrum was recorded, and aliquots of a stock solution of CoCp$_2$ were added using a stop-loc syringe.

Electrochemistry. Electrochemical measurements were performed using an electrochemical system for cyclic voltammetry, phase sensitive *ac* polarography, and *dc* polarography. It consisted of a fast rise-time potentiostat,[46] a lock-in amplifier (Stanford Research, model SR830), a digital storage osciloscope (LeCroy, model Scope Station 310), and a synthesized function generator (Stanford Research, model DS340). The instruments were interfaced to a personal computer via an IEEE-interface card (PC-Lab, AdvanTech model PCL-848) and a data acquisition card (PCL-818) using 12-bit precision. A three-electrode electrochemical cell was used. The reference electrode, Ag|AgCl|1 M LiCl, was separated from the test solution by a salt bridge, and the half-wave potential of ferrocene against it was +0.65 V. The working electrode for voltammetry and *ac* polarography was a valve-operated static mercury electrode (SMDE2, Labo-

ratorní Přístroje, Prague) with an area of 1.13×10^{-2} cm^2. The working electrode for *dc* polarography was a glass capillary connected to a mercury reservoir (column height 45 cm) with an outflow rate of 1.06 mg/s. The drop time of 1 s was mechanically regulated. The working electrodes for voltammetry at fast scan rates were gold or platinum disks with diameters 10, 25, 50, and 500 μm sealed in glass. The auxiliary electrode was a cylindrical platinum net. The reduction products were prepared by exhaustive electrolysis of 1×10^{-3} mol L^{-1} solutions in THF or in acetonitrile. The cell for electrolysis was made of two compartments for the working and auxiliary electrodes, separated by a 10 cm long salt bridge with a sintered glass junction. To eliminate any traces of water, molecular sieve was added to cell compartments. Exhaustive electrolysis was performed on a mercury pool cathode at a potential corresponding to a selected limiting diffusion current. Oxygen was removed from the solution by a stream of argon. Spectroelectrochemical data were recorded in an optically transparent thin-layer cell using a diode array UV−vis spectrometer (Hewlett-Packard, model 8452A).

EPR Spectroscopy. A solution of **2a** was produced in THF (2 mL) containing the CB$_{11}$Me$_{12}$$^-$ salt of **1a**, obtained by ion exchange in ethyl acetate from 0.5 mg of the triflate salt (3×10^{-7} mol). It was freeze−thaw degassed in a sidearm reservoir of a ~3 mm OD glass or quartz ESR tube and flushed with argon and reduced by addition through a septum of a few microliters of a solution of cobaltocene in THF (1.0 mg/mL, 5.3×10^{-3} M), prepared under argon atmosphere. It was stable for at least several hours. The spectrum was obtained with a Bruker ESP 300E X-band spectrometer (modulation frequency, 12.5 kHz; amplitude, 1.46 G; time constant, 1.25 ms; and conversion time, 10.24 ms). A combination of a large modulation amplitude and a small modulation frequency was chosen to achieve good sensitivity without excessive line broadening [the hyperfine structure of p-(NMe$_2$)$_2$C$_6$H$_4$$^+$ was resolved under similar conditions]. Simulation of the five-line pattern was performed using SimFonia 1.25 software and yielded a coupling constant of 2.6 ± 0.1 G and a line width of 2.7 G (two equivalent ^{14}N nuclei with $I = 1$, 1:1 Lorentzian/Gaussian ratio).

A virtually identical EPR spectrum was recorded in acetonitrile when **2a** was prepared either by electrolysis of **1a** followed by a sample transfer to a cell or by a direct electrolytic generation on a mercury meniscus inside a thin quartz cell, using an ERS-220 spectrometer (Centre for Production of Scientific Instruments, Academy of Sciences of GDR, Berlin, Germany) operated by a CU-1 unit (Magnettech, Berlin, Germany) in the X-band. The g value was determined using a Mn^{2+} standard at $g = 1.9860$ (MI = 1/2 line).

Titration experiments with simultaneous measurement of UV−vis and EPR spectra were performed in THF and acetonitrile using similar procedures. The cobaltocene was assayed in dry solvents under argon by oxidation with iodine, addition of tetrabutylammonium iodide, and potentiometric back-titration of excess iodine with aqueous thiosulfate and was found to be nearly 100% pure. The solutions used in the titration were standardized against aqueous primary standards (K$_2$Cr$_2$O$_7$ and Na$_2$S$_2$O$_3$).

Results

The choice of the terminal substituents in **1** has little effect on the results, and we describe primarily those obtained with **1a**.

Choice of Solvent. While the salts of **1** are soluble in many solvents, the higher oligomers are soluble in highly polar
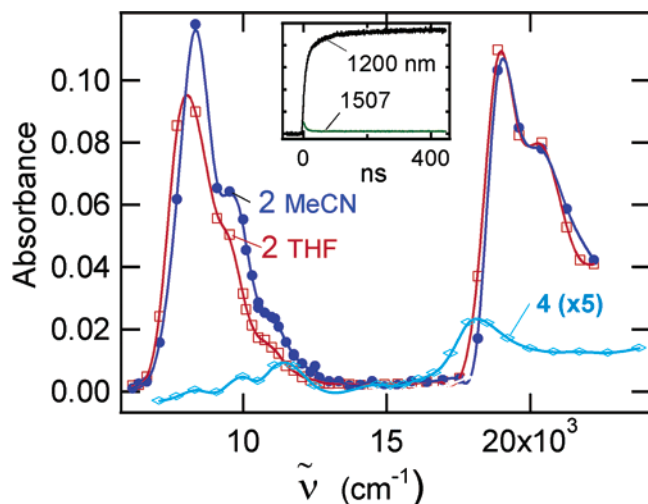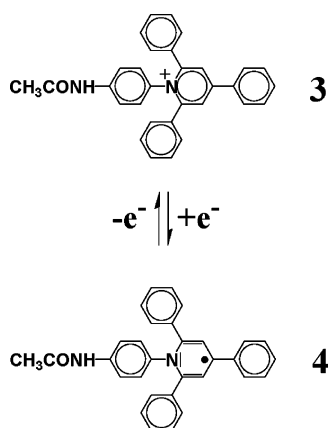
One-Electron Reduction of an Extended Viologen

J. Phys. Chem. A, Vol. 109, No. 48, 2005 **10865**

Figure 1. Transient absorption spectra at 200 ns formed upon electron attachment to **1a** ($CB_{11}Me_{12}^-$ salt) by pulse radiolysis in acetonitrile (MeCN) and THF. The inset shows the growth of **2a** at 1200 nm and the decay of solvated electrons at 1507 nm in acetonitrile containing 1 mM **1a**. Bottom: the spectrum formed upon reduction of **3** to **4** by electrons in MeCN (Scheme 2), scaled by a factor of 5.

SCHEME 2

Figure 2. Absorbance changes induced by reduction of **1a** ($CB_{11}Me_{12}^-$ salt) with Na metal in THF. The spectra are labeled by the time of contact of the solution with metal surface; the redox equivalents added are not known except by inference from the results.

Figure 3. Absorption spectra during a redox titration of 40 μM **1a** ($CB_{11}Me_{12}^-$ salt) in THF with CoCp$_2$. The spectra are labeled by values of $n = [CoCp_2]/[1a]$. Spectra for $n = 0-1.0$ are shown blue, then green to $n = 2$, and red for $n > 2$.

solvents (DMSO) regardless of the choice of counterion and in low-polarity solvents (THF) with the $CB_{11}Me_{12}^-$ counterion. We have tested the reduction of **1** in some very polar solvents (DMSO, MeCN) and some of lower polarity (THF, CH_2Cl_2). We found that in CH_2Cl_2 the one-electron reduction product **2a** is unstable, presumably because this solvent is irreversibly reduced too easily, and eliminated it from further consideration. In dry THF or THF-d_8, **2a** is stable for at least tens of minutes in the absence of oxygen, and we have chosen this solvent for a detailed investigation. Traces of moisture lead to secondary transformations, presumably triggered by an initial protonation, and we have taken extreme measures to avoid this complication.

Reduction of 1a in THF by Pulse Radiolysis. Pulse radiolysis of THF produces solvated electrons (e_s^-) absorbing in the near-IR. This strongly reducing species reacts rapidly with **1a** with a rate constant $(4.2 \pm 1.5) \times 10^{11}$ M^{-1} s^{-1} to form a species **2a** characterized by absorption peaks at 494, 535, and 1245 nm (Figure 1).

Reduction of 1a in THF with Na Metal. The same spectrum was obtained when **1a** was reduced by contact with Na metal (Figure 2). The strong band peaking at 535 nm gives the solutions of **2a** a red color. Repeated contact with Na increased the absorption bands of **2a**, while bleaching of **1a** was observed at 340 nm. After the fifth contact (60 s), **1a** was 90% bleached, suggesting that ~0.9 reducing equivalents had been introduced
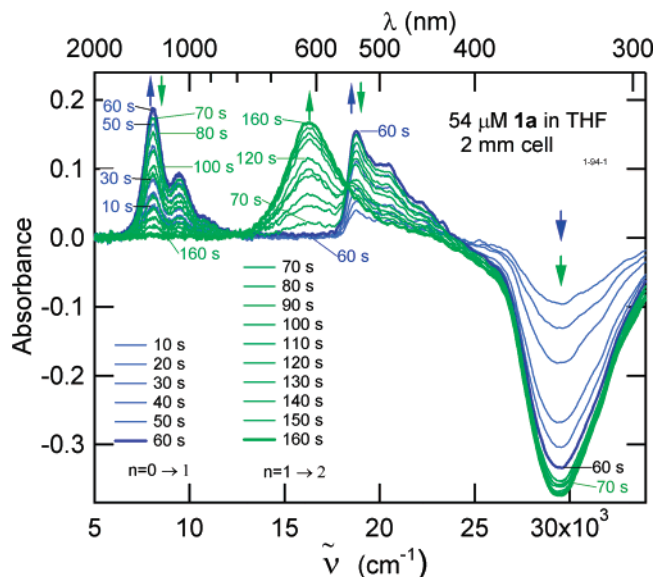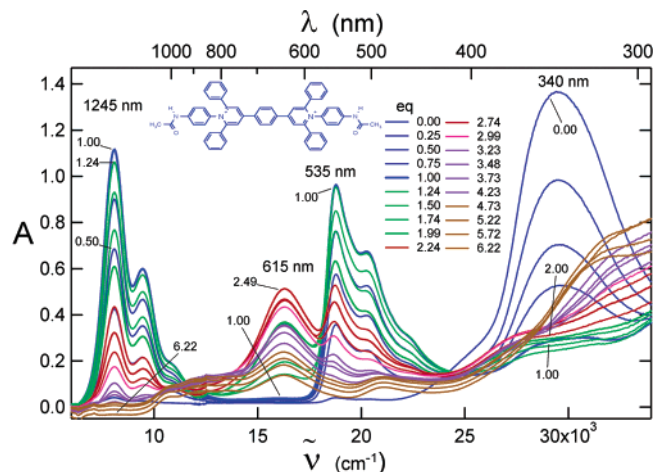
at that point (see below). Upon further exposure to Na, the bands of **2a** decreased, and a new band grew at 615 nm. With sufficient contact, the red **2a** disappeared entirely, and the 615 nm species gave the solution a blue color.

Reduction of 1 in THF with Cobaltocene. The extended viologen **1a** can also be reduced by cobaltocene, **1a** + CoCp$_2$ → **2a** + CoCp$_2^+$ (Cp = C_5H_5). For this reaction, unlike reduction by Na, the number of equivalents n of the reducing agent per **1a** is precisely known. Figure 3 plots the absorption spectra as a function of n. The visible and NIR bands of the red **2a** increase to a maximum at $n = 1.0$, where 97% of the 340 nm band of parent **1a** is removed. Above $n = 1.0$, the bands of **2a** decrease and the 615 nm band attributed to the blue species grows. A low-temperature spectrum of **2a** is shown in Figure 4, and the course of titration in the presence of added electrolyte is shown in Figure 5.

The titration experiment with cobaltocene was repeated many times. In some of these experiments, UV−vis−NIR and EPR spectra were both measured on the same solutions. During the whole process of conversion of **1a** into the red species **2a** and
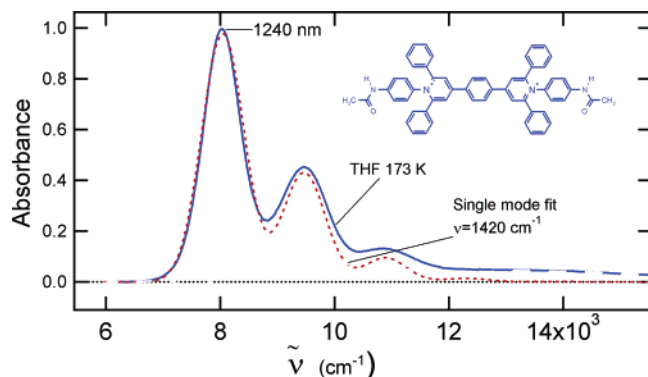
Figure 4. Near-IR absorption of **1a** ($CB_{11}Me_{12}^-$ salt) reduced with $CoCp_2$ in THF at 173 K and a fit to a single mode Franck−Condon progression.

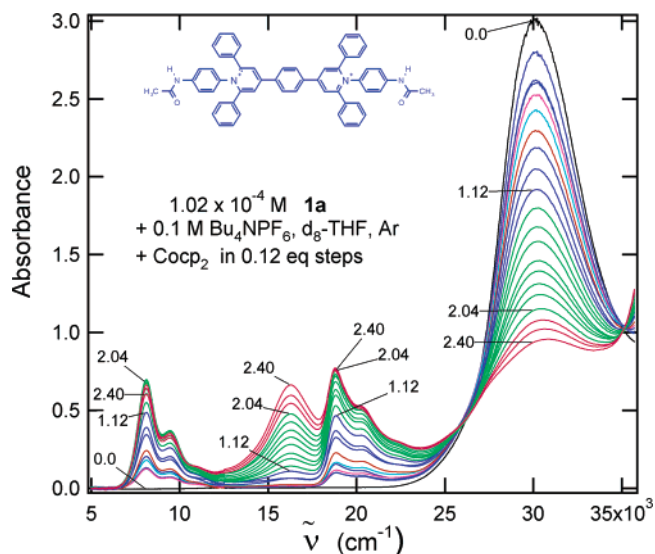**Figure 5.** Absorption spectra during a redox titration of 102 μM **1a** ($CB_{11}Me_{12}^-$ salt) with $CoCp_2$ in THF in the presence of 0.1 M tetrabutylamonium hexafluorophosphate.

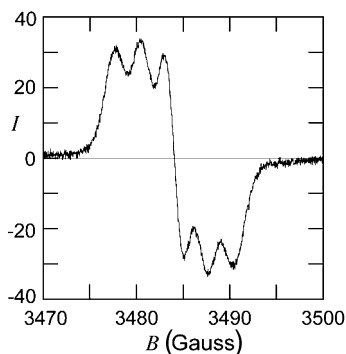**Figure 6.** EPR spectrum of red solution of **1a** ($CB_{11}Me_{12}^-$ salt) obtained by reduction with cobaltocene in THF. The spectrum obtained by electrolysis in acetonitrile at −0.8 V is the same.

its subsequent destruction by conversion to the blue species after more than one equivalent of $CoCp_2$ is added, the solution showed the same EPR signal (Figure 6), whose intensity was proportional to the height of the visible and near-IR absorption peaks. The spectrum consists of a 1:2:3:2:1 quintet of broad lines with a coupling costant of 2.6 G. The starting **1a** and the blue product absorbing at 615 nm were EPR silent.

When the titration with cobaltocene was performed in the presence of 0.1 M tetrabutylammonium hexafluorophosphate (Figure 5), the red species **2a** was again formed first, but the
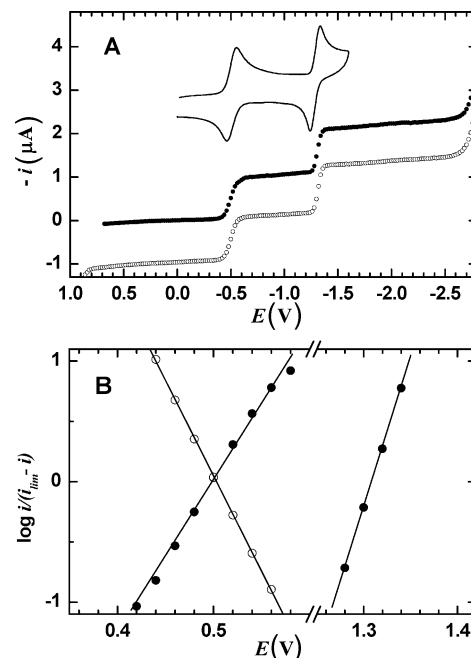

Figure 7. (A) Dc polarography of 1 mM **1a** (triflate salt) in 0.1 M tetrabutylamonium hexafluorophosphate in THF on mercury drop electrode (drop time 1 s). Full points, before electrolysis; hollow circles, after exhaustive electrolysis at the potential of the limiting diffusion current of the first wave (−0.8 V). Cyclic voltammogram on a glassy carbon electrode at the scan rate 0.1 V/s (full line) is offset for better visibility. (B) Log-plot analysis of waves before and after the electrolysis, using the same point symbols as in panel A.

band at 615 nm started to appear slightly earlier, being noticeable at $n = 0.96$. In contrast to the experiment without added electrolyte, the bands of **2a** did not decrease with addition of more $CoCp_2$ even up to $n = 1.8$ equivalents, after which a gradual decrease was seen to $n = 2.4$.

Electrochemical Reduction of 1a in THF. These studies were performed on a dropping mercury electrode in the presence of 0.1 M tetrabutylammonium hexafluorophosphate. The dication **1a** is reduced in two separate reversible one-electron steps at half-wave potentials of −0.50 and −1.31 V, as can be seen on a *dc* polarogram (Figure 7A). The limiting currents of the first and the second reductions of a 1 mM solution are 10% lower than the limiting current of 1 mM ferrocene, demonstrating that each wave is due to a one-electron reduction. The reversible and one-electron nature of the redox process was confirmed by cyclic voltammetry (Figure 7A) and by the slope of log-plot analysis of the shape of the polarographic current−voltage curve (Figure 7B).

The one-electron nature of the first wave at −0.5 V was further verified by repeated exhaustive electrolysis at constant potentials adjusted to values from −0.7 to −0.9 V. Charge consumption per mole of **1a** needed for reduction at the potential of the limiting current of the first wave was identical with that obtained by exhaustive electrolysis of methyl viologen. The *dc* polarogram of the reduced sample showed an anodic wave at −0.50 V and a cathodic wave at −1.31 V (Figure 7A). Reduced solutions could be reoxidized by electrolysis or by admission of oxygen.

During the course of electrolysis at potentials of the first reduction wave, the solution color quickly changed to red and turned to blue only at the end. These color changes are documented by spectroelectrochemical measurements in an optically transparent thin-layer cell (Figure 8). The potential
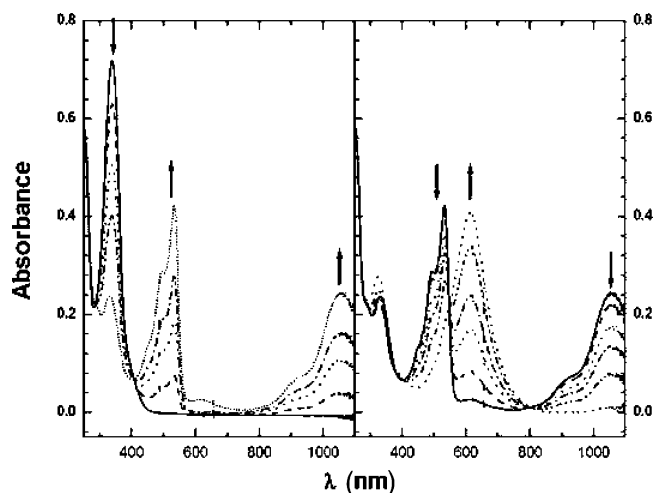
One-Electron Reduction of an Extended Viologen

J. Phys. Chem. A, Vol. 109, No. 48, 2005 **10867**

Figure 8. Spectroelectrochemistry of 0.78 mM **1a** (triflate salt) and 0.05 M LiCB$_{11}$Me$_{12}$ in THF. Spectra in the left panel correspond to potentials −0.45 (full line), −0.56, −0.57, −0.58, −0.59, and −0.61 V. Spectra in the right panel correspond to potentials −0.62 (full line), −0.64, −0.655, −0.675, −0.69, and −0.75 V. Arrows indicate the change in band intensities when a more negative potential is applied.

scan through the region to the first reduction step in THF showed a gradual decrease of the absorption band of the dication at 340 nm and the appearance of bands at 494 and 535 nm corresponding to the red one-electron reduction product **2a**. When the electrode potential approached the diffusion plateau of the first polarographic wave (half-wave potential, −0.5 V), absorption bands at 494 and 535 nm gradually disappeared and were replaced by the 615 nm band of a blue species (Figure 8).

Reduction of 1 in Other Solvents. The presence of a supporting electrolyte, required in electrochemical measurements to ensure proper solution conductivity, may cause ion pairing to play a role in solvents of low dielectric permittivity. Therefore, many of our experiments were also repeated in acetonitrile and DMSO.

Pulse radiolysis in acetonitrile yields solvated electrons, possibly in equilibrium with another strongly reducing species, believed to be (MeCN)$_2^-$.[47−50] These reductants reacted rapidly with **1a** and gave results virtually identical with those obtained in THF (Figure 1). The near-IR peak is slightly shifted and narrowed relative to THF. The rate constant for electron attachment was $(7.2 \pm 2) \times 10^{10}$ M^{-1} s^{-1} in MeCN.

All electrochemical observations described above remained the same also in acetonitrile and DMSO. In particular, the one-electron nature of the first wave (at −0.5 V) was verified thoroughly by repeated exhaustive electrolysis at constant potentials adjusted to values from −0.7 to −0.9 V. A comparison with the limiting currents of 1 mM methyl viologen solution in acetonitrile yielded equal current values.

However, in acetonitrile and DMSO, visual observations as well as spectroelectrochemical measurements showed that the characteristic absorption bands of the red species **2a** appear only at the initial stages of exhaustive electrolysis at potentials within the range of the first reduction wave, until the absorption peak of **1a** near 340 nm decreased by about ∼20%. At higher conversions, the red species **2a** spontaneously transforms into a blue species with an absorption band at 615 nm that appears identical with the band observed in chemical overreduction of **1a**. This occurs even at reduction potentials at which slow-scan electrochemical measurements yield no evidence of an acceptance of a second electron.

Voltammetry at a sufficiently high scan rate should be able to suppress or eliminate the effect of the chemical reactions

that transform the primary red reduction product **2a** to the blue species in these solvents. Indeed, voltamograms recorded on ultramicroelectrodes at scan rates between 100 and 10 000 V/s permitted us to detect a reduction process that is not seen at slow scan rates (Figure 9) and led to an estimate of the true second redox potential of **1a** as about −0.9 V instead the value −1.31 V that one would infer from Figure 7. This value is more negative than the first reduction step by approximately the same amount as the separation of the two redox potentials of methyl viologen.

Steady state voltammograms of **1a** were also recorded on a 10 μm Pt electrode in the absence of a supporting electrolyte in acetonitrile. The resulting current−voltage curves showed the same features and shapes as the polarogram given in Figure 7.

The slow-scan electrochemical behavior is qualitatively the same for all four choices of terminal substituents, but the choice of substituent and of solvent influences the potentials of the second reduction step somewhat more than that of the first. In acetonitrile, the first reduction potentials are −0.64 (**1a**), −0.66 (**1b**), −0.60 (**1c**), and −0.62 (**1d**) V, whereas under slow-scan conditions the values for the second reduction wave are −1.33 (**1a**), −1.43 (**1b**), −1.37 (**1c**), and −1.27 (**1d**) V.

Discussion

All pulse radiolytic, chemical, and electrochemical evidence agrees that the red species **2** is the monomeric cation radical produced by one-electron reduction of **1** as represented in Scheme 1. Perhaps not surprisingly in view of the complex redox chemistry of viologens discussed briefly in the Introduction, the nature of the blue product responsible for the 615 nm band remains uncertain at this time. The results of chemical reduction experiments suggest that the blue compound is a doubly reduced form of **1**, and rapid scan results agree that such a species is formed at −0.9 V (Figure 8) and is accessible. In contrast, electrochemical results suggest that the blue compound is a dimer of the red compound **2**. Possibly, there are two blue compounds with similar absorption spectra. We prefer to obtain additional experimental evidence before attempting a structural assignment. Fortunately, the nature of the blue product is not directly relevant to the issue at hand, one-electron doping of the extended viologen molecular wires.

The pulse radiolytic rate constants for electron attachment to **1a** are larger than those typical for diffusion-controlled reactions with neutral solutes. This is attributed to its positive charges, one of which is probably compensated by ion pairing in THF. Diffusion-controlled reactions with neutral solutes are typically a factor of 3 slower in MeCN and a factor of 5−10 slower in THF. The rapidity of these attachment processes is an advantage: **2a** is created 5−10 times faster than any of its possible following reactions with the parent **1**, ensuring that the primary reduction product is observed.

The red cation radical **2a** is stable in THF in the absence of oxygen, and exhaustively reduced samples can be electrochemically reoxidized by removal of one equivalent of electrons. The redox system **1/2** is reversible and exhibits fast kinetics. Because reduced viologens are known to participate frequently in follow-up reactions such as dimerizations, the pulse radiolysis results are especially useful for a safe identification of the primary reduction product. Given that the Lambert−Beer law for **1a** had been verified over a large concentration range[1] and that there is no indication that the solute is anything but monomeric **1a**, the identification of the red species **2a** as monomeric, singly reduced **1a** is beyond doubt. The EPR spectrum of the red form
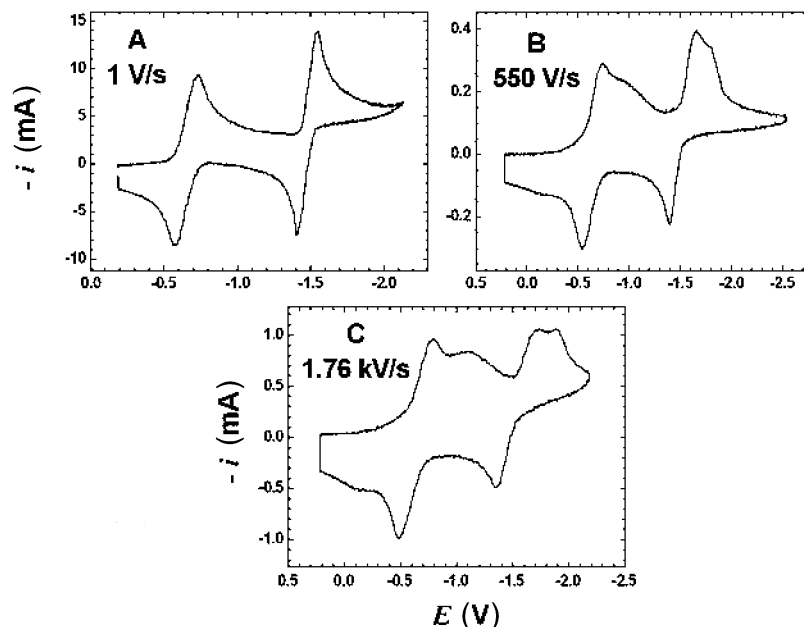
Figure 9. Cyclic voltammetry of 9 mM **1b** (triflate salt) and 1 M tetrabutylamonium hexafluorophosphate in acetonitrile. The working electrode was a gold disk with a diameter of (A) 0.5 mm and (B,C) 25 μm. The scan rates are indicated.

also confirms that **2a** is singly reduced **1a**. The nature of this one-electron reduced molecule will be important in understanding possible charge transport in oligomers containing two or more conjugated repeat units of **1**. The reduction potential, 0.25 V more negative than that of methyl viologen, is favorable for the use of these oligomers as semiconductor wires of the *n* type.

A distinctive feature of the optical absorption spectrum of **2** is the strong absorption band peaking at 1245 nm in the near-IR. Its slight shift and narrowing in acetonitrile relative to THF are plausibly attributed to reduced ion pairing. The fine structure is suggestive of vibrational sublevels.

Near-IR "intervalence" or "optical electron transfer" (OET) bands often occur upon single electron reduction or oxidation of molecules having two reduction or oxidation sites such as the two pyridinium groups in **1**. An OET could occur between localized states centering on the two pyridiniums, analogous to Robin–Day class I intervalence transitions in metal complexes.[51] The molecule would then exist in two interconverting forms. Because the two pyridiniums are identical, such an OET band would have its origin at zero photon energy and increase steadily to a maximum at the reorganization energy for electron transfer. Such bands are usually broad and featureless due to the large contribution of solvation to the reorganization energy.

The near-IR transition of **2a** is clearly not such an OET band and shows that the representation shown in Scheme 1, with only one molecular species described by two resonance structures, is correct. Optical absorption in Figures 1–5 has little or zero intensity below 7000 cm^{-1} and then rises rapidly to the sharp peak at 1245 nm (8000 cm^{-1}). While OET bands are typically devoid of resolved vibrational structure, the near-IR band of **2a** shows pronounced structure. The low-temperature spectrum agrees well with the computed Franck–Condon progression for a displaced oscillator with a frequency of 1420 cm^{-1} and a reorganization energy of 770 cm^{-1} (Figure 4). Small departures from the simple single-mode approximation occur with increasing vibrational excitation, probably indicating weak coupling to vibrations of other frequencies. The room temperature spectrum (Figure 3) is also described well by the same progression if the width of each vibrational band is increased. The resolved vibrational structure is typical of transitions

between delocalized states in which the charge distribution changes relatively little between the two states. The delocalized nature of **2** is also compatible with the EPR spectrum, which shows that the two nitrogen atoms are equivalent, at least on the EPR time scale.

These observations show that **2a** has an electronic gap of 8000 cm^{-1} between its ground and excited states. Such a gap is typically observed when electronic coupling between states localized on the two halves of a molecule is strong enough to delocalize the electron over both halves, in our case stabilizing the ground state by half of 8000 cm^{-1}. Gas phase calculations on **2a** by the ZINDO (INDO/S)[52,53] semiempirical MO method predicted a somewhat lower energy transition between a symmetric delocalized ground state and an antisymmetric excited state at 5500 cm^{-1}.

The near-IR transition at 8000 cm^{-1} is approximately a factor of 2 lower in energy than the comparable transition at 740 nm or 13500 cm^{-1} (maximum at 610 nm, 16400 cm^{-1}) in reduced methyl viologen,[13,16] reflecting weaker electronic coupling between the two pyridinium halves, now coupled through the intermediacy of a benzene ring. If **1** is viewed as two coupled "half-viologens", reduction of **1** (to **2**) would be expected to be easier by ~4000 cm^{-1} than the reduction of an isolated half. The cation **3** is clearly only an imperfect model for such an isolated half, but it shows roughly the expected behavior, and its reduction potential to yield the radical **4** is 310 mV (2500 cm^{-1}) less positive than that of **1**. The disagreement is plausibly due to differences in solvation energies, which are larger in **3/4** than in **1/2**, and to the effect of the acetamido substituent. The cation radical **2a** can thus be described as stabilized by an ~4000 cm^{-1} delocalization energy, which is ~60% of that in MV$^{+\bullet}$.

The NIR bands of **2** are also much sharper than the ~600 nm bands of reduced methyl viologen (MV$^{+\bullet}$). In **2**, the lowest energy (8000 cm^{-1}) vibrational line is the tallest, while in MV$^{+\bullet}$ the lowest energy band is relatively small, with the tallest band, that at ~600 nm, being perhaps the third. This implies that structural changes (reorganization) upon promotion to the allowed excited state are much smaller in **2** than in MV$^{+\bullet}$. While other factors undoubtedly contribute, one reason is apparent. Optimization of MV$^{+\bullet}$ leads to a planar structure, enforced by

One-Electron Reduction of an Extended Viologen

J. Phys. Chem. A, Vol. 109, No. 48, 2005 **10869**

occupancy of the symmetric (b_{3u}) SOMO. Promotion to the excited state, on the other hand, places the electron in an antisymmetric (b_{2g}) orbital with a node at the center of the inter-ring C–C bond. This excited state will likely twist even more than the parent compound, MV^{2+}, which optimizes (ZINDO) to a structure with a 45° inter-ring angle. In **2**, the ground state is also symmetric and the excited state is antisymmetric, but the node is at the center of the middle benzene ring and the occupation of this orbital does not result in large torsional changes between the ground and the excited states.

Conclusions

The extended viologen unit **1** accepts an electron in a fast and reversible process, yielding the cation radical **2**, in which the added electron is fully delocalized. The oligomers of **1** appear worth investigating for possible use as *n*-semiconducting molecular wires.

References and Notes

(1) Valášek, M.; Pecka, J.; Jindřich, J.; Calleja, G.; Craig, P. R.; Michl, J. *J. Org. Chem.* **2005**, *70*, 405.
(2) Berlin, Y. A.; Hutchison, G. R.; Rempala, P.; Ratner, M. A.; Michl, J. *J. Phys. Chem. A* **2003**, *107*, 3970.
(3) Makowski, M. P.; Mattice, W. L. *Polymer* **1993**, *34*, 1606.
(4) Harris, F. W.; Chuang, K. C.; Huang, S. A. X.; Janimak, J. J.; Cheng, S. Z. D. *Polymer* **1994**, *35*, 4940.
(5) Huang, S. A. X.; Chuang, K. C.; Cheng, S. Z. D.; Harris, F. W. *Polymer* **2000**, *41*, 5001.
(6) Lin, F.; Cheng, S. Z. D.; Harris, F. W. *Polymer* **2002**, *43*, 3421.
(7) Sun, X.; Yang Y.-k.; Lu, F. *Polymer* **1999**, *40*, 429.
(8) Efimova, E. V.; Lymar, S. V.; Parmon, V. N. *J. Photochem. Photobiol. A* **1994**, *83*, 153.
(9) Haiss, W.; van Zalinge, H.; Höbenreich, H.; Bethell, D.; Schiffrin, D. J.; Higgins, S. J.; Nichols, R. J. *Langmuir* **2004**, *20*, 7694.
(10) Raymo, F. M.; Alvarado, R. J.; Pacsial, E. J.; Alexander, D. *J. Phys. Chem. B* **2004**, *108*, 8622.
(11) Leventis, N.; Yang, J.; Fabrizio, E. F.; Rawashdeh, A.-M. M.; Oh, W. S.; Sotiriou-Leventis, C. *J. Am. Chem. Soc.* **2004**, *126*, 4094.
(12) Michaelis, L. *Biochem. Z.* **1932**, *250*, 564.
(13) Kosower, E. M.; Cotter, J. L. *J. Am. Chem. Soc.* **1964**, *86*, 5524.
(14) Thorneley, R. N. F. *Biochim. Biophys. Acta* **1974**, *333*, 487.
(15) Roullier, L.; Laviron, E. *Electrochim. Acta* **1977**, *22*, 669.
(16) Watanabe, T.; Honda, K. *J. Phys. Chem.* **1982**, *86*, 2617.
(17) Novakovic, V.; Hoffman, M. Z. *J. Am. Chem. Soc.* **1987**, *109*, 2341.

(18) Volke, J.; Dunsch, L.; Volkeová, V.; Petr, A.; Urban, J. *Electrochim. Acta* **1997**, *42*, 1771.
(19) Imabayashi, S.-I.; Kitamura, N.; Tokuda, K.; Tazuke, S. *Chem. Lett.* **1987**, 915.
(20) Imabayashi, S.-I.; Kitamura, N.; Tazuke, S.; Tokuda, K. *J. Electroanal. Chem.* **1988**, *239*, 397.
(21) Mohammad, M. *Electrochim. Acta* **1988**, *33*, 417.
(22) Pospíšil, L.; Kůta, J.; Volke, J. *J. Electroanal. Chem.* **1975**, *58*, 217.
(23) Pospíšil, L.; Kůta, J. *J. Electroanal. Chem.* **1978**, *90*, 231.
(24) Beden, B.; Enea, O.; Hahn, F.; Lamy, C. *J. Electroanal. Chem.* **1984**, *170*, 357.
(25) Scharifker, B.; Wehrmann, C. *J. Electroanal. Chem.* **1985**, *185*, 93.
(26) Heyrovský, M.; Novotný, L. *Collect. Czech. Chem. Commun.* **1987**, *52*, 1097.
(27) Kokkinidis, G.; Hasiotis, C.; Papanastasiou, G. *J. Electroanal. Chem.* **1993**, *350*, 235.
(28) Kitamura, F.; Ohsaka, T.; Tokuda, K. *J. Electroanal. Chem.* **1993**, *347*, 371.
(29) Millán, J. I.; Sánchez-Maestre, M.; Camacho, L.; Ruiz, J. J.; Rodríguez-Amaro, R. *Langmuir* **1997**, *13*, 3860.
(30) Millán, J. I.; Amaro, R. R.; Ruiz, J. J.; Camacho, L. *J. Phys. Chem. B* **1999**, *103*, 3669.
(31) Stargardt, J. F.; Hawkridge, F. M. *Anal. Chim. Acta* **1983**, *146*, 1.
(32) Ito, M.; Sasaki, H.; Takahashi, M. *J. Phys. Chem.* **1987**, *91*, 3932.
(33) Lee, C.; Kim, C.; Moon, M. S.; Park, J. W. *Bull. Korean Chem. Soc.* **1994**, *15*, 909.
(34) Alden, J. A.; Cooper, J. A.; Hutchinson, F.; Prieto, F.; Compton, R. G. *J. Electroanal. Chem.* **1997**, *432*, 63.
(35) Tam, K. Y.; Wang, R. L.; Lee, C. W.; Compton, R. G. *Electroanalysis* **1997**, *9*, 219.
(36) Webster, R. D.; Dryfe, R. A. W.; Eklund, J. C.; Lee, C.-W.; Compton, R. G. *J. Electroanal. Chem.* **1996**, *402*, 167.
(37) Norton, J. D.; White, H. S. *J. Electroanal. Chem.* **1992**, *325*, 341.
(38) Amatore, C.; Bento, M. F.; Montenegro, M. I. *Anal. Chem.* **1995**, *67*, 2800.
(39) Amatore, C.; Bonhomme, F.; Bruneel, J.-L.; Servant, L.; Thouin, L. *J. Electroanal. Chem.* **2000**, *484*, 1.
(40) Das, T. N.; Ghanty, T. K.; Pal, H. *J. Phys. Chem. A* **2003**, *107*, 5998.
(41) King, B. T.; Janoušek, Z.; Grüner, B.; Trammell, M.; Noll, B. C.; Michl, J. *J. Am. Chem. Soc.* **1996**, *118*, 3313.
(42) Kostanecki, v. St.; Rossbach, G. *Ber. Dtsch. Chem. Ges.* **1896**, *29*, 1488.
(43) Hirsch, S. S.; Bailey, W. J. *J. Org. Chem.* **1978**, *43*, 4090.
(44) Wishart, J. F.; Cook, A. R.; Miller, J. R. *Rev. Sci. Instrum.* **2004**, *75*, 4359.
(45) Miller, J. R.; Penfield, K.; Johnson, M.; Closs, G.; Green, N. In *Advances in Chemistry Series*; Wishart, J. F., Nocera, D. G., Eds.; American Chemical Society: Washington, DC, 1998; Vol. 254, pp 161–176.
(46) Pospíšil, L.; Fiedler, J.; Fanelli, N. *Rev. Sci. Instrum.* **2000**, *71*, 1804.
(47) Bell, I. P.; Rodgers, M. A. J.; Burrows, H. D. *J. Chem. Soc., Faraday Trans. I* **1977**, *73*, 315.
(48) Shkrob, I. A.; Sauer, M. C., Jr. *J. Phys. Chem. A* **2002**, *106*, 9120.
(49) Shkrob, I. A.; Takeda, K.; Williams, F. *J. Phys. Chem. A* **2002**, *106*, 9132.
(50) Xia, C.; Peon, J.; Kohler, B. *J. Chem. Phys.* **2002**, *117*, 8855.
(51) Brunschwig, B. S.; Creutz, C.; Sutin, N. *Chem. Soc. Rev.* **2002**, *31*, 168.
(52) Ridley, J. E.; Zerner, M. C. *Theor. Chim. Acta* **1976**, *42*, 223.
(53) Bacon, A. D.; Zerner, M. C. *Theor. Chim. Acta* **1979**, *53*, 21.